ACS APPLIED MATERIALS & INTERFACES

Research Article

www.acsami.org

High-Performance Piezoresistive Electronic Skin with Bionic Hierarchical Microstructure and Microcracks

Pu Nie,[†,‡] Ranran Wang,[*,†] Xiaojuan Xu,[†,‡] Yin Cheng,[†,‡] Xiao Wang,[†,‡] Liangjing Shi,[†] and Jing Sun[*,†]

[†]State Key Laboratory of High Performance Ceramics and Superfine Microstructure, Shanghai Institute of Ceramics, Chinese Academy of Sciences, 1295 Ding Xi Road, Shanghai 200050, People's Republic of China

[‡]University of Chinese Academy of Sciences, 19 Yuquan Road, Beijing 100049, People's Republic of China

Supporting Information

ABSTRACT: Electronic skin (E-skin), a popular research topic at present, has achieved significant progress in a variety of sophisticated applications. However, the poor sensitivity and stability severely limit the development of its application. Here, we present a facile, cost-effective, and scalable method for manufacturing E-skin devices with bionic hierarchical microstructure and microcracks. Our devices exhibit high sensitivity (10 kPa^{-1}) and excellent durability (10 000 cycles). The synergistic enhancement mechanism of the hierarchical microstructure and the microcracks on the conductive layers was discovered. Moreover, we carried out a series of studies on the airflow detection and the noncontact speech recognition.

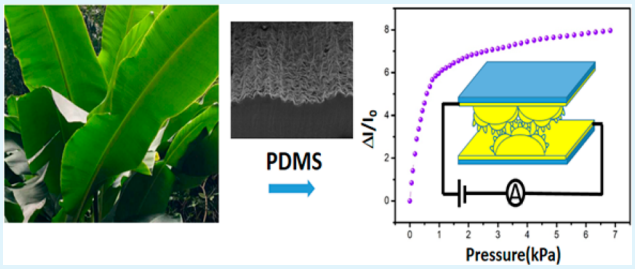

KEYWORDS: *electronic skin, hierarchical microstructure, microcrack, bionic, banana leaf*

1. INTRODUCTION

Recently, substantial research enthusiasm has been directed to electronic skin (E-skin).[1−3] Human skin, as the body's largest organ, can convert external signals, such as pressure, temperature, and other complex environmental stimuli, to the physiological electrical signals and transfer them to the brain, enabling us to feel such stimuli.[4−6] Much progress has been made to develop E-skin devices to promote wide use in the field ranging from wearable electronics, real-time health monitoring, to highly intuitive human−computer user interfaces and intelligent robots.[7−11] These explorations have promoted rapidly increasing innovations of E-skin with great scientific significance and application prospect.

Pressure sensors with improved performance are mainly based on three physical transduction mechanisms,[12] including piezoresistivity,[13−17] capacitance,[18−20] and piezoelectricity.[21,22] Among them, piezoresistive sensors have been widely studied because of their simple device structure, readout mechanism, and high sensitivity, one of the most important performance parameters of E-skin.[14−17,23,24] Piezoresistive E-skin is composed of two main parts: one is the flexible substrate usually formed by polydimethylsiloxane (PDMS), due to its so many excellent characteristics, such as good elastic properties, desirable biocompatibility, and easy micropatterning,[25−27] and another is the sensing material, which mainly includes carbon nanotubes, graphene, and metal nanowires. To obtain highly sensitive E-skin devices that can mimic and even outperform the subtle pressure sensing capabilities of human skin, many measures have been explored, such as capacitive sensors with micropyramid array,[19] piezoresistive sensors with Pt-coated interlocking nanofibers,[28] and AuNWs-coated tissue paper,[29] tunneling piezoresistive sensors with interlocked microdome arrays,[30] and flexible polymer transistors with microstructured PDMS.[31] Among the above examples, microstructured PDMS with special microfeatures, which has smaller shape factor,[32] can deform more easily because of the concentrated stress as compared to PDMS with a flat and smooth surface, therefore tremendously improving its mechanical properties and pressure-responsive behaviors. Bao's group[19,31,33] developed different types of E-skin with pyramid patterned PDMS, which exhibited a short response time and excellent cycling stability. Fan et al.[34] reported self-powered pressure sensors based on pyramid patterned PDMS films with a low detection limit of ∼13 mPa. The microstructured PDMS films mentioned above were fabricated by copying the structure of patterned Si molds, produced by time-consuming photolithography at high cost. Many groups developed a variety of methods to obtain low-cost and easily prepared micropatterned PDMS films. Wang et al.[13] even tried to replicate the microstructure of silk surface to fabricate PDMS films and further assembled piezoresistive E-skin devices with favorable performance, the sensitivity of which is as high as 1.8 kPa^{-1} and the detection limit is 0.6 Pa.

As compared to monotonous microstructure, hierarchical structure is prone to give rise to a more rapid increase of the contact areas when pressure is loaded, thus improving the sensitivity and sensing range of E-skin. However, it is difficult to fabricate molds with hierarchical structure on the micro/submicro scale through the photolithography method. Leaves

Received: February 10, 2017
Accepted: April 12, 2017
Published: April 12, 2017

DOI: 10.1021/acsami.7b01979
ACS Appl. Mater. Interfaces 2017, 9, 14911−14919

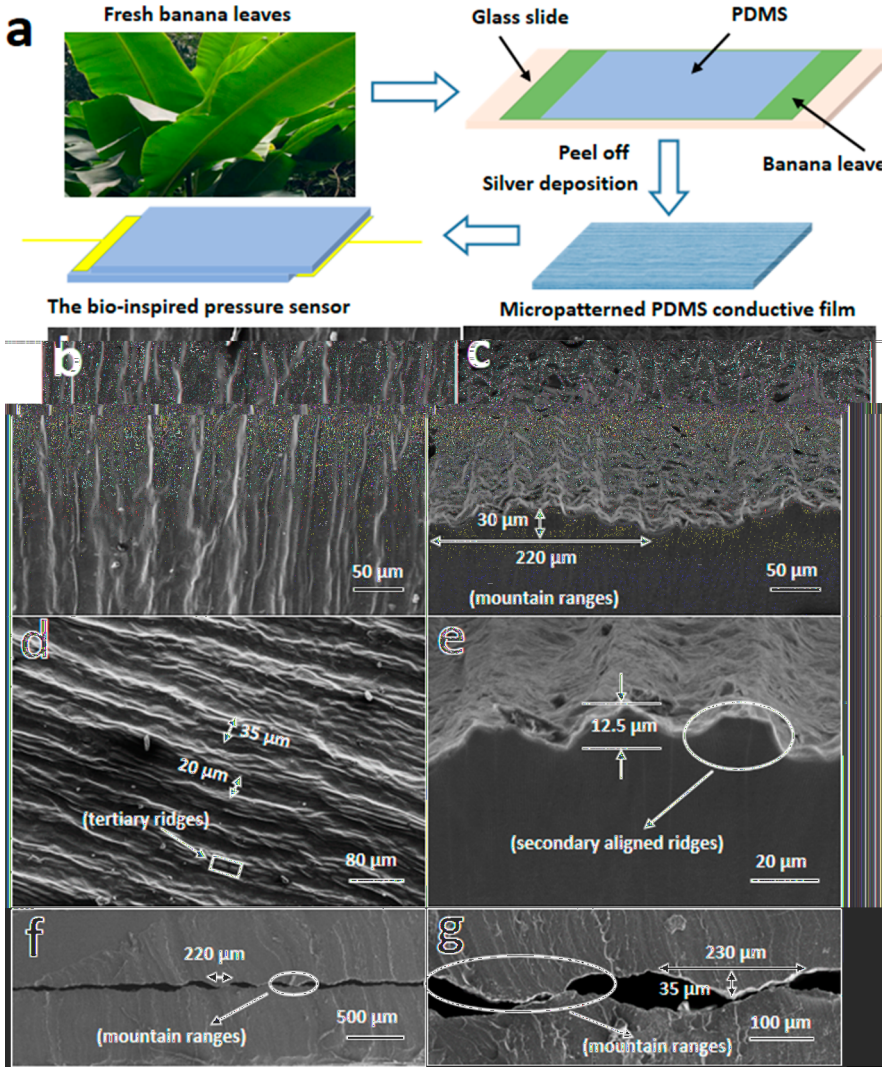

Figure 1. (a) Schematic illustration of the fabrication process of flexible PDMS films and corresponding pressure sensors. (b–e) SEM images of flexible PDMS electrode with the inverted microstructure of banana leaves. (b,d) Top view and 10° view, respectively. (c,e) Cross sections of the micropatterned PDMS electrode. (f,g) Cross sections of the micropatterned E-skin device.

are not only the most significant functional organs of plants, but also one of the most sensitive organs to external environment changes. In the long-term evolution, nature endows plant leaves fascinating morphologies with a high degree of structure heterogeneity and unique function to adapt to the constantly changing environment. Therefore, leaves have been chosen as the natural molds for constructing subtle microstructures to enhance the sensitivity of E-skin. Cheng[16] and Liu et al.[35] reported a two-step negative/positive molding method to mold PDMS with mimosa and rose petal, respectively, and assembled E-skin devices. However, only monotonous microstructures were patterned, and the devices exhibited low sensitivity.

Herein, PDMS substrate patterned with aligned mountain ranges with secondary and tertiary ridges on the micrometer scale was fabricated by replicating the hierarchical microstructure of the surface of banana leaves. Thin silver layer was deposited upon the microstructured PDMS surface to work as the sensing electrode of the piezoresistive E-skin, and microcracks formed in the layer under pressure. The hierarchical microstructure and the microcracks enhance the sensitivity of the E-skin synergistically, which endow the device with high sensitivity of 10 kPa^{-1} when pressure is less than 400 Pa, and 3.3 kPa^{-1} in the pressure range of 400–1000 Pa. Besides, E-skin with the novel structure also demonstrated a low detection limit (~1 Pa), short response time and low relaxation time (36 and 30 ms), and great stability (>10 000 cycles). The superior performance enabled the E-skin device to detect gas flow with ultralow flow rate, based on which noncontact voice recognition and human breath gas flow monitoring were realized. Moreover, extensive applications in such human physiological signals as voice recognition, wrist pulse monitoring, and muscular movement were also demonstrated.

2. RESULTS AND DISCUSSION

Device Fabrication. The overall fabrication procedure is shown in Figure 1a. A fresh and clean banana leaf was used as the mold to fabricate micropatterned PDMS thin films. After the PDMS solution was poured onto the banana leaves template, solidified, and then peeled off, a PDMS film with inverse microstructure of the leaves template was easily gained (the thickness of the PDMS films was kept as ~200 μm). The surface morphologies of the patterned PDMS films were observed by SEM (Figure 1b–e), which assemble like parallel

DOI: 10.1021/acsami.7b01979
ACS Appl. Mater. Interfaces 2017, 9, 14911–14919

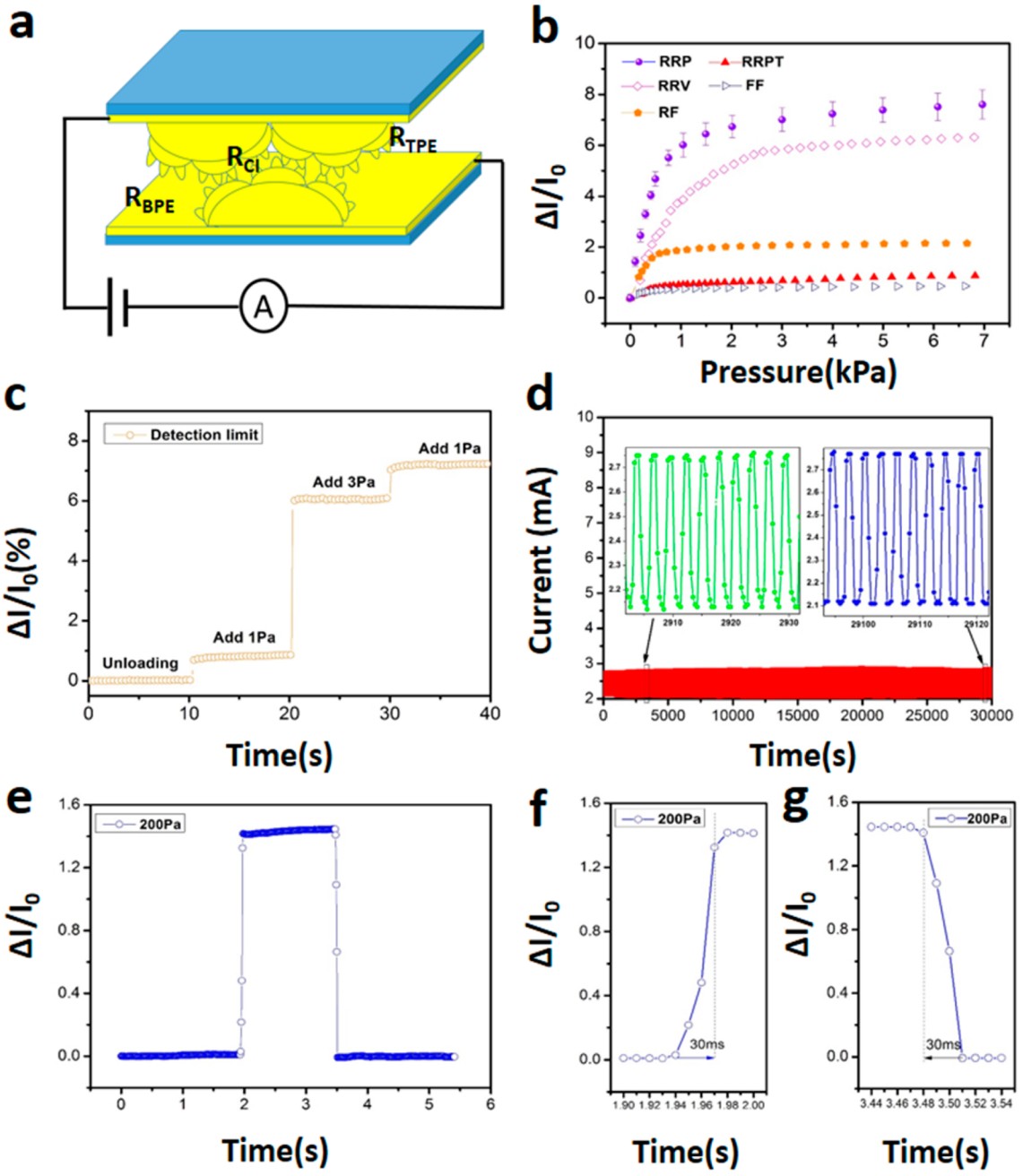

Figure 2. Pressure sensing properties of the pressure sensor with high-sensitivity, low detection limit, stability, and short response time. (a) Schematic diagram of the E-skin. (b) Pressure−response curves for different types of E-skin devices. (c) Real-time $I-t$ curves of the E-skin for detection of three small glasses, 30, 90, and 30 mg, respectively. (d) Real-time $I-t$ curves of the E-skin for more than 10 000 loading/unloading cycles, at 3 s for each cycle, with an applied pressure of 1 kPa. (e−g) Short response and relaxation time of the E-skin.

mountain ranges with uniform secondary aligned ridges on which are tertiary ridges of different shapes and sizes. The width of parallel mountain ranges is ∼220 μm (Figure 1c,f,g), and the height is ∼30 μm (Figure 1c,g). The distance between each adjacent secondary aligned ridge on the primary mountain-like structure is ∼20 μm, the width is ∼35 μm (Figure 1d), and the height is ∼12 μm (Figure 1e). The tertiary ridges on the secondary aligned ridges look like a rectangular microconvex with area ranging from several to hundreds square micrometers.

To make the microstructured and flexible PDMS substrates surface conductive, a thin layer of conducting silver film (∼50 nm thick) was deposited upon the rough surfaces. The thickness of conductive silver layer was investigated. Thinner ones (∼25 nm) showed very poor conductivity as well as low resistance change, while their counterparts (∼100 nm) exhibited stable resistance and low responsive impedance. Therefore, a 50 nm thick silver layer was the chosen thickness in this study.

Herein, the highly sensitive E-skin sensor was assembled using two PDMS flexible electrodes with micropatterned surfaces placed face-to-face that formed an interlocked construction, while copper wires were anchored on the edge of both films with silver paste. The distinctive microstructure made the external stimuli concentrate on very limited areas, and thus a great change in resistance would appear even under low

DOI: 10.1021/acsami.7b01979
ACS Appl. Mater. Interfaces 2017, 9, 14911−14919

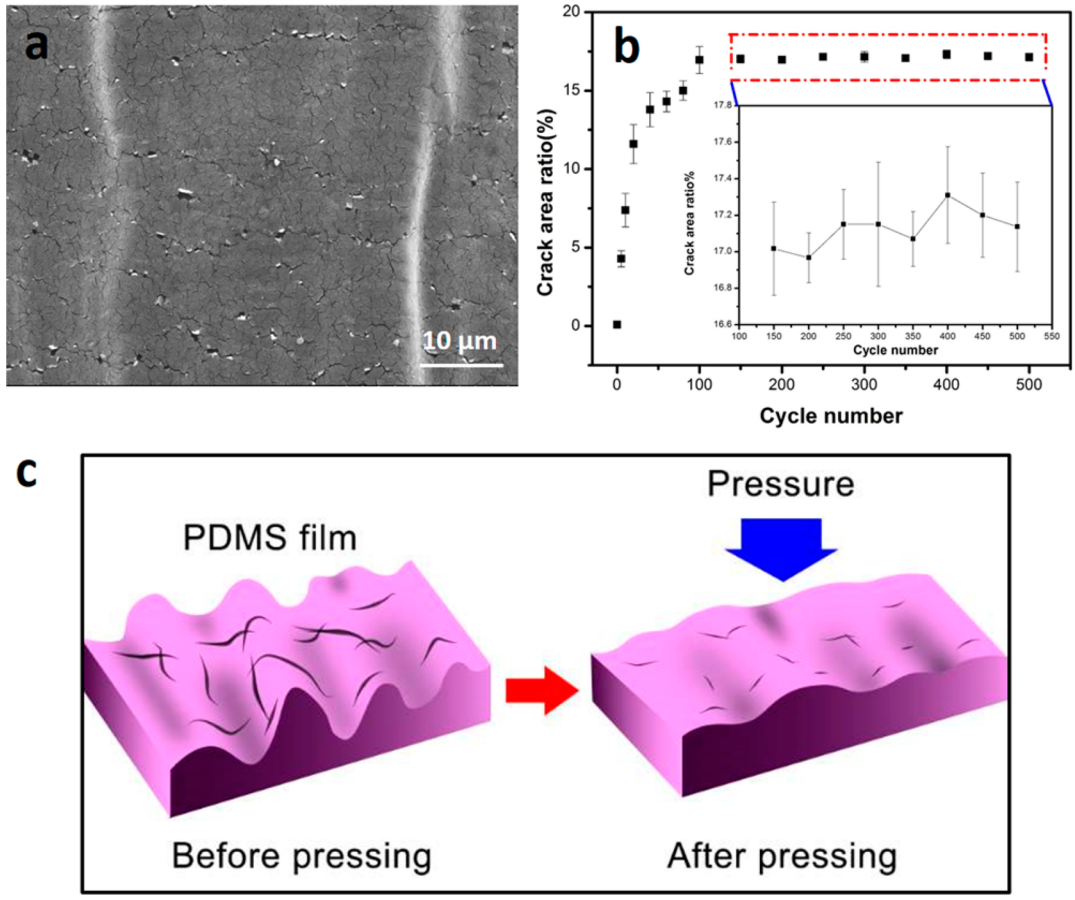

Figure 3. (a) SEM image of the PDMS flexible electrode after 10 000 cycles (applied pressure 1 kPa, 3 s for each cycle). The crack area proportion is 16.41%. (b) The crack area of the PDMS flexible electrode occupies the proportion of the whole area at different loading/unloading cycles (3 s for each cycle, with an applied pressure 1 kPa). (c) Schematic illustration of microstructure deformation and dynamic change process of the crack before and after pressing.

pressure. To study the effect of microstructure and the configuration on the sensing performance, five different types of E-skin sensors were designed, which were rough-to-rough surfaces parallelly interlocked (RRP), rough-to-rough surfaces vertically interlocked (RRV), rough-to-flat surfaces interlocked (RF), rough-to-rough surfaces parallelly interlocked with thicker conductive films (~100 nm) (RRPT), and flat-to-flat surfaces interlocked (FF) (schematic illustration of different configurations in Figure S1).

Following the method reported by Bao's group,[19] a thin rectangular glass slide (20 mm × 30 mm, 1.52 g) was placed over the entire device to facilitate the pressure sensing test. The pressure produced by the glass slide is defined as "base pressure" for the sensor, and additional pressure is defined as "applied pressure". The sensitivity (S) of the bioinspired E-skin was tested by utilizing a computer-controlled stepping motor and a force gauge. The sensitivity S can be defined as

$$S = \frac{\delta\left(\frac{\Delta I}{I_0}\right)}{\delta P} \quad (1)$$

$$\Delta I = I - I_0 \quad (2)$$

where I is the current of the sensor with applied pressure, while I_0 is the current with only base pressure on the device, ΔI is the relative change in current, and P is the applied pressure. The relative current change ($\Delta I/I_0$) can better characterize the pressure response of this piezoresistive type sensor than the resistance ratio term ($\Delta R/R_0$) (eqs S1 and S2). We could find that E-skin of RRP type shows the highest sensitivity; RRV type also demonstrates high sensitivity, but it is lower than that of RRP type, as shown in Figure 2b. The other three types of sensor are insensitive to the applied pressure in the range from 1 to 7 kPa. It is obvious that the special structure on the PDMS film greatly enhances the pressure sensitivity of the sensor as compared to the unstructured film. Consequently, E-skin of RRP type has been detailedly investigated in this work.

To understand the resistive response of the E-skin devices, a simple circuit model was developed, as shown in Figure 2a. The resultant resistance (R) around aligned ridges is the sum of three parts: the resistances of the top piezoresistive electrode (R_{TPE}), contact interface (R_{CI}), and bottom piezoresistive electrode (R_{BPE}), as given in eq 3:

$$R = R_{TPE} + R_{CI} + R_{BPE} \quad (3)$$

Because of the complex hierarchical microstructure of the biotemplates, the sensitivity curves exhibit three linear parts: the sensitivity of the device is 10 kPa^{-1} in the low pressure region (0−400 Pa), 3.3 kPa^{-1} (400−1000 Pa), and 0.33 kPa^{-1} (1−7 kPa). The high sensitivity is due to the hierarchical microstructure. As shown in Figure 2a, when the pressure is applied, first, tertiary ridges begin to contact closely and then deform. Next, the secondary aligned ridges and primary mountain ranges experience similar changes with the increase

DOI: 10.1021/acsami.7b01979
ACS Appl. Mater. Interfaces 2017, 9, 14911−14919

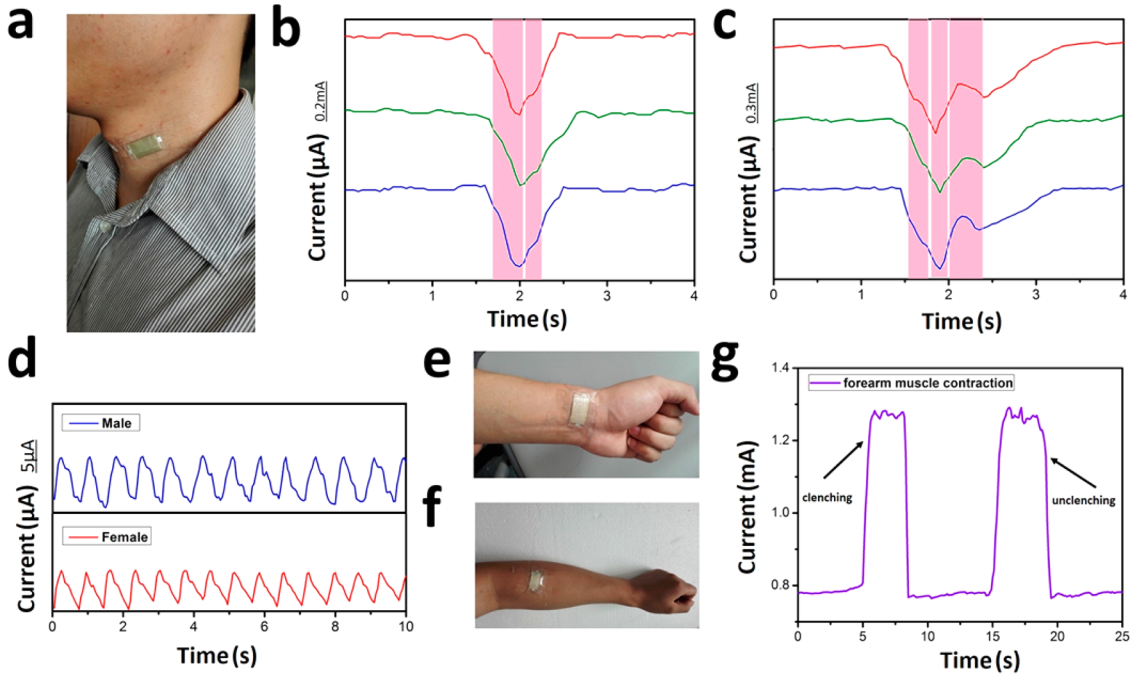

Figure 4. (a) Photograph of the E-skin directly attached to a volunteer's neck for monitoring the muscle movement during speaking. (b,c) Real-time *I*–*t* curves of the E-skin in response to different voices saying "Hi", "Let's go". (d) Real-time *I*–*t* curves for monitoring wrist pulses of a man and a woman. (e) Photograph of the E-skin for the detection of wrist pulses. (f) Photograph showing the detection of forearm muscle contraction. (g) Current variation of the forearm muscle contraction induced by clenching and unclenching fist.

of pressure. Because of the sensitive pressure response of small structures, a small pressure stimuli can induce large current variation, which explains the high sensitivity. The contact area between the two electrodes tends to saturate in high pressure range, and the applied pressure plays no part in the current variation, and therefore the sensitivity decreases.

To further demonstrate the capability of as-prepared flexible pressure sensors to sense a tiny amount of pressure, three small glasses (30, 90, 30 mg) were loaded in proper order (Figure 2c). The high sensitivity indicates that the device is very suitable for detecting very small pressure. The corresponding pressure of the three glasses were 1, 3, and 1 Pa, respectively. Such a low detection limit benefited from the good pressure response of tertiary ridges on the hierarchically microstructured electrodes. Another important advantage of the micropatterned sensor was its durability. To further investigate the working stability of the pressure sensor, the current changes of the device were obtained when repeatedly loading/unloading applied pressure of 1 kPa for more than 10 000 cycles (3 s for each cycle), as illustrated in Figure 2d. The cyclic test results demonstrated the high repeatability, stability, and durability of the device. Figure 2e shows the response and relaxation times are 36 and 30 ms. The rapid response time of our E-skin is very close to that of real human skin (30–50 ms),[36] because of the immediate change of the contact area of microconvex when pressure is applied and removed. The short response time originated from the microstructures on the PDMS thin films, which provide voids that enable the rough surfaces to elastically deform on application of external pressure, thus decreasing the residual hysteresis effect from the compression and relaxation times of entangled PDMS polymer chain.[19]

Similar to many results reported previously,[37−39] we also found repeated external pressure loading on our E-skin device results in emerging of cracks in the rigid conducting layers upon the PDMS surfaces (Figure 3 and Figure S2). It is believed that such cracks should have significant effects on the sensing performance of our device. As seen from Figure S3, the initial current dropped significantly in the first 10 cycles, and then turned stable gradually. Differently, the current output when loaded to the critical value (about 10 kPa) remained almost unchanged after each cycle. We attributed the drop and stabilization of the initial current to the growth, propagation, and saturation of cracks in loading cycles, and called this the activation process. To demonstrate this, we carried out cycling tests 500 times (applied pressure 1 kPa, 3 s for each cycle), and the microstructure of the silver layer on the PDMS rough surface was studied at the 0, 5th, 10th, 20th, 40th, 60th, 80th, 100th, 150th, 200th, 250th, 300th, 350th, 400th, 450th, and 500th cycle. The crack area under different cycles was calculated with Image-pro plus software (Figure 3 and Figure S2). Cracks in the picture were dyed red (Figure S2). We calculated the area proportion of the red area using Image-pro plus. As seen from Figure 3b, the crack area proportion increases within 100 cycles and then remains stable, which indicates that cracks of rigid conducting silver layers stop propagating after a certain number of external stimuli. This observation coincides with the variation of the initial current within the primeval 100 cycles. The appearance and propagation of irreversible cracks reduces the area of electron pathways, thus leading to the drop of initial current. After that, cracks stop propagating and hold steady, which accounts for the stabilization of initial current. When loading, the microconvex on the PDMS substrate would deform. The height of the convex would decrease, while the width would increase, which led to the coalescence of the microcracks, as shown in Figure 3c. Consequently, the damaged electron pathways were rebuilt. Therefore, the influence of the propagation of cracks was eliminated under the critical loading condonation, which

DOI: 10.1021/acsami.7b01979
ACS Appl. Mater. Interfaces 2017, 9, 14911−14919

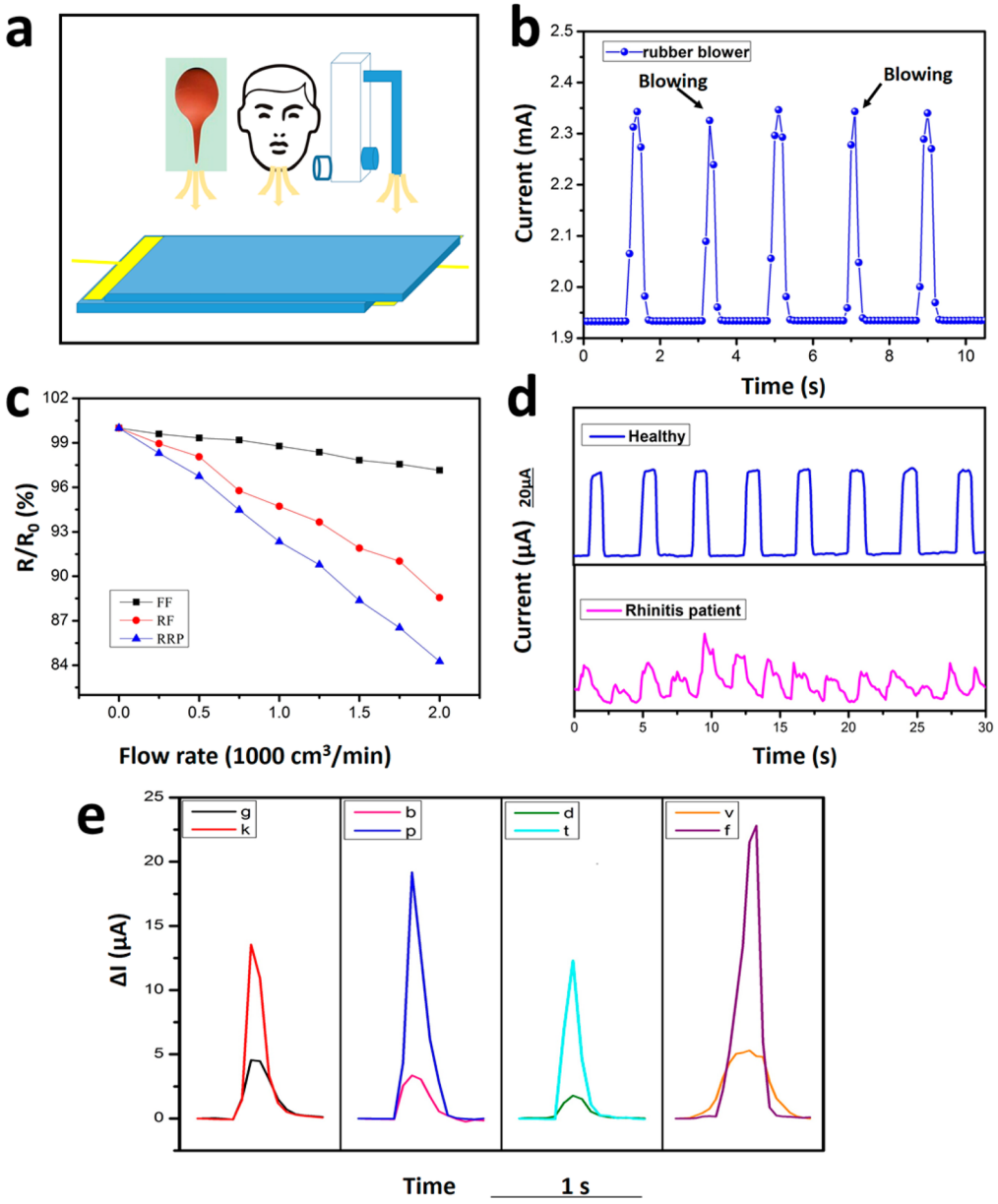

Figure 5. Monitoring of gas flow and human breathing without directly contacting. (a) Schematic of a rubber blower blowing air, human breathing, and gas flow sensing for the E-skin device. (b) Current signal peaks in response to the rubber blower. (c) Relative changes in current as a function of flow rate. (d) Relative current changes in monitoring of a healthy human breathing and a rhinitis patient breathing. (e) Real-time $I-t$ curves of the E-skin when monitoring gas flow during the tester's speech.

explains the negligible difference of the current output when loaded to the critical value (about 10 kPa).

All in all, the cracks on the PDMS flexible substrate, which divided the conductive film into a series of islands in a pattern often seen in drying mud, had the following advantage to construct E-skin devices: these microcracks can improve the corresponding E-skin's current response. They would significantly reduce the initial current (I_0) due to the destruction of conductive pathways to a certain extent in the absence of applied pressure, and the coalescence of the microcracks when loading would lead to a greater sense of current signal as compared to those without microcracks on the conductive layers. Thus, we made full use of the cracks appearing on the E-skin device instead of avoiding it in this work.

The working mechanism of the device was dominated by both pressing-force-dependent contact area change between top and bottom rough surfaces and the variation of crack width. A small compressive deformation of microstructured PDMS surfaces generated when an external pressure stimuli was applied; thus the contact area between the two electrodes would increase and the microcracks would coalesce, resulting in larger charge transfer and corresponding resistance decrease. When the pressure was removed, these microspots of the patterned PDMS films would return to the original state and the microcracks would broaden, reducing the contact area between the two electrodes and increasing the width of microcracks, thus leading to the recovery of the resistance to the primary value. Therefore, the exceedingly good electricity-responsive behaviors of the flexible pressure sensor are almost entirely attributed to the following two factors: (1) hierarchical micro/nanostructured patterns on the interface of two Ag-film/PDMS electrodes provided far more effective contact sites and

DOI: 10.1021/acsami.7b01979
ACS Appl. Mater. Interfaces 2017, 9, 14911−14919

much better pressure response than those without special patterns; and (2) coalescence and broadening of the microcracks on the rigid conducting layers upon PDMS surfaces endowed our device with much better current sensing performance. Unlike flexible electrodes without microcracks, even very small pressure loading on the device can generate distinct current variation due to the coalescence of the microcracks, which causes excellent sensing signals for our E-skin.

The E-skin devices can be tailored to appropriate size for different pressure sensing applications. We stuck the E-skin (1.5 × 2 cm^2) on a volunteer's neck to monitor the muscle movement when talking to demonstrate the sensing capability (Figure 4a). As illustrated in Figure 4b and c, the $I-t$ curves of the E-skin exhibit distinct patterns when the volunteer spoke different words and short sentences, such as "Hi" and "Let's go", respectively. Every word or sentence was recorded three times to investigate the repeatability. It is observed that three $I-t$ curves have similar shapes when the volunteer said the same word or short sentence. The sensitivity and repeatability of voice recognition are mainly caused by the vibration of epidermis and muscles around the throat during speech. The effective monitoring of voices makes the E-skin promising candidates for electronic-skin applications such as speech recovery training and human−machine interaction.[13]

The E-skin can be placed over the radial artery of the wrist to detect subtle pressure caused by blood pressure to demonstrate the potential of the device in disease diagnosis; pulse wave signal is one of the important signals that can reflect the physical condition of the body (Figure 4e). As shown in Figure 4d, the typical characteristics of wrist pulses were collected containing early systolic peak pressure (P-wave), late systolic peak pressure (T-wave), and diastolic pulse waveform (D-wave),[40] demonstrating a low detection limit of the E-skin and its potential application in physiological diagnosis. Besides, we can also find that P-wave of a man is faster and stronger, meaning a greater momentum of blood ejection as compared to that of a woman.[13] Research shows that the time delay between the P-wave(t_1) and T-wave(t_2) ΔT_{DVP} ($=t_2 - t_1$) and the radial augmentation index AIr (=T-wave/P-wave) are two of the most commonly used parameters for arterial stiffness diagnosis. Here, for the two test persons, ΔT_{DVP} = 200−250 ms and AIr = 50−60% have been determined, a reflection of the good health of the persons.[31,41]

To further explore the sensitivity and flexibility of the sensor, the bionic microstructured sensor was used to detect human muscular movement (Figure 4f). Muscular movement of clenching fist deformed the sensor pasted on skin, and thus the current signals could be detected with high sensing capability (Figure 4g).

Beyond the application for touch sensing, here, the sensor is also able to detect noncontact actions (Figure 5). We used the device to detect the blowing generated by the rubber blower, shown in Figure 5b. Notable sensing signal was detected when the blower was gripped. The air flowing out of the blower transmits the action triggers to pressure stimuli without direct contact during the detecting. On the basis of this, the nontouching E-skin could be extended to potential applications like vibration monitoring, turbulent flow detection, gas flow detection,[30] acoustic transducer, and so on. As schematically depicted in Figure 5a, gas flow on the E-skin's surface can cause low pressure that deformed the interlocked microconvex and imparted a decrease in resistance. This value of R_{on}/R_{off} decreases linearly with an increase in flow rate (0−1.2 m s^{-1}) (Figure 5c). We find the E-skin with interlocked microstructure is more sensitive to airflow than others. Conversely, the FF type E-skin exhibit a low sensitivity. This can also demonstrate that bionic microstructure of the electronic skin greatly improves resistance response.

Furthermore, we put the E-skin device under the nostrils of a volunteer, and the amount of air exhaled was measured to investigate the potential for using the device to monitor human breathing (Figure 5a and d). As depicted in Figure 5d, the periodic breathing generates repeatable and stable variation in current for a healthy person, and every breath event results in 40 μA change in current. However, test results show that the rhinitis patient's breath is quicker, weaker, and disorganized. That is because rhinitis patients' noses are easy to block and breath is difficult for them; therefore, their breath is not regular and more rapid to make up the insufficiency of the oxygen demand. The experimental results indicate that our high-sensitive sensor could be suited as breathing sensors in diagnosis and rehabilitation of respiratory diseases. Furthermore, we put the E-skin device on the test desk, and a person spoke to the device; thus a burst of air induced by speaking was measured to investigate the potential application for noncontact voice recognition, which is a little different from Park's work in which the noncontact speech recognition was realized by a speaker.[42] As illustrated in Figure 5e, voiceless consonants p, t, k, and f produced much larger current variation than voiced consonants b, d, g, and v, which is attributed to the different phonation mod; when we read the voiceless consonant, the vocal cords are not vibrating and the corresponding air flow is strong, thus causing a larger current change, while the case is opposite when we read the voiced consonants. Yet when multisyllable words were read, distinct current signals were obtained only in the stressed syllables. Although our electronic skin cannot complete complex noncontact speech recognition, we believe that noncontact speech recognition will be realized when E-skin's sensitivity is high enough and the response time is short enough, which will help patients with their vocal cord removed to regain the ability to speak.

3. CONCLUSIONS

In summary, we have developed supersensitive, rapid-responding, and reliable E-skin devices by combining micropatterned PDMS substrate with microcracked Ag ultrathin films. The hierarchical microstructure was obtained by mimicking banana leaves and enhanced the sensitivity of the E-skin device greatly. Microcracks in the conducting layer aroused from pressure also improved the sensitivity of the device. The synergistic response mechanism was proposed. Moreover, the applications of the E-skin devices in monitoring voice recognition, real-time wrist pulse detection, muscular movement, airflow detection, human breathing, and noncontact speech recognition have been shown with great sensing performance. Importantly, the whole fabrication process of the E-skin device is facile, low-cost, and environmentally friendly. We believe that versatile fabrication methodology provides a new way for the fabrication of high-performance E-skin device with a wide range of applications in future cost-effective wearable electronics.

4. EXPERIMENTAL SECTION

Fabrication of Banana Leaves Molded Microstructured PDMS Conducting Films. First, the banana leaves were cut into

DOI: 10.1021/acsami.7b01979
ACS Appl. Mater. Interfaces 2017, 9, 14911−14919

sizes of 3 × 1.5 cm^2 (try to select large leaves and avoid the thick veins) and washed with deionized water for 10 min, then washed with ethanol twice and dried with a hair dryer to get pieces of precleaned plant leaves templates, which were attached to clean glasses very flatly by double faced adhesive tape.

Second, the fabrication of micropatterned PDMS flexible film is performed. The PDMS solution mixture of prepolymer and the curing agent (Dow Corning Sylgard 184; the weight ratio of prepolymer to the curing agent was 10:1) was stirred at least for 10 min, and placed for a period of time at room temperature until the bubbles disappear. The PDMS mixture then was poured onto the leaves mold. The remaining air bubbles between the PDMS and template were removed in a vacuum drying oven to make a great replicate of the microstructure. After being heated at 80 °C for 4 h, fortunately, micropatterned PDMS thin film was easily peeled off from the leaves template because of the low surface energy. Flat PDMS films were produced by slide template.

Third, to make the PDMS rough surface conductive, Ag coating (thickness ~50 nm) was thermally evaporated through a shadow mask under vacuum (3 × 10^{-3} Pa). Finally, banana leaves molded microstructured PDMS conducting films were obtained.

Fabrication of Flexible E-Skin. The bioinspired flexible pressure sensor was constructed by two flexible PDMS conductive films with rough surfaces placed face-to-face, extracted by copper wires that were glued on one border of the Ag films with silver paste. After the silver paste dried at room temperature for an hour, two flexible films of the E-skin devices were overlapped together with each other (silver paste electrode not touching the surface of the other film). Finally, the edges of the device were bonded with adhesive tape, yielding the generation of high-performance flexible pressure sensors.

Characterization. The micromorphology of the micropatterned PDMS surface was accomplished with a field-emission scanning electron microscope (Hitachi S-4800).

The $I-t$ curves in real-time of the E-skin were measured using an electrochemical workstation (PARSTAT2273, Princeton Applied Research).

The resistance of the device when testing gas flow was measured by a two-probe method with a FLUKE-15B digital multimeter, and the rate of gas flow was controlled by a rotameter.

The force applied on the E-skin was detected by a force gauge (Handpi Digital force gauge, HP5).

The sensitivity of the E-skin was measured by a high precision electronic universal testing machine (CMT6103, MTS Systems (China) Co., Ltd.) and a force gauge. The force (F) and current (I) were recorded. Here, the pressure (P) was calculated by $P = F/A$, where A is the forced area.

The durability of the E-skin was measured by a movable stage (ZXT_050-300_MA06 (China), Shanghai Zhengxin Optio-electrical Technology Co. Ltd.)

■ ASSOCIATED CONTENT

Supporting Information

The Supporting Information is available free of charge on the ACS Publications website at DOI: 10.1021/acsami.7b01979.

Explanation of the relative current change ($\Delta I/I_0$) to better characterize the pressure response of this piezoresistive type sensor than the resistance ratio term ($\Delta R/R_0$), schematic illustration of the configurations of four different E-skin devices, study on the distribution of crack area on the PDMS flexible electrodes after 0, 10, 80, and 100 loading/unloading cycles, real-time $I-t$ curves of the E-skin for the initial 30 times sensitivity test, and real-time $I-t$ curves of the E-skin for the first 1200 loading/unloading cycles and after 12 000 loading/unloading cycles (PDF)

■ AUTHOR INFORMATION

Corresponding Authors

*E-mail: wangranran@mail.sic.ac.cn.
*E-mail: jingsun@mail.sic.ac.cn.

ORCID

Jing Sun: 0000-0003-1101-1584

Notes

The authors declare no competing financial interest.

■ ACKNOWLEDGMENTS

This work was financially supported by the National Key Research and Development Program of China (2016YFA0203000), Shanghai Science and Technology Star Project, Youth Innovation Promotion Association CAS (2014226), The Shanghai Key Basic Research Project (16JC1402300), and The State Key Lab of High Performance Ceramics and Superfine Microstructure Director fund.

■ REFERENCES

(1) Choi, S.; Lee, H.; Ghaffari, R.; Hyeon, T.; Kim, D.-H. Recent Advances in Flexible and Stretchable Bio-Electronic Devices Integrated with Nanomaterials. *Adv. Mater.* **2016**, *28* (22), 4203−4218.

(2) Kim, S. Y.; Park, S.; Park, H. W.; Park do, H.; Jeong, Y.; Kim, D. H. Highly Sensitive and Multimodal All-Carbon Skin Sensors Capable of Simultaneously Detecting Tactile and Biological Stimuli. *Adv. Mater.* **2015**, *27* (28), 4178−4185.

(3) Zhu, B.; Niu, Z.; Wang, H.; Leow, W. R.; Wang, H.; Li, Y.; Zheng, L.; Wei, J.; Huo, F.; Chen, X. Microstructured graphene arrays for highly sensitive flexible tactile sensors. *Small* **2014**, *10* (18), 3625−3631.

(4) Zimmerman, A.; Bai, L.; Ginty, D. D. The gentle touch receptors of mammalian skin. *Science* **2014**, *346* (6212), 950−954.

(5) Raspopovic, S.; Capogrosso, M.; Petrini, F. M.; Bonizzato, M.; Rigosa, J.; Di Pino, G.; Carpaneto, J.; Controzzi, M.; Boretius, T.; Fernandez, E.; Granata, G.; Oddo, C. M.; Citi, L.; Ciancio, A. L.; Cipriani, C.; Carrozza, M. C.; Jensen, W.; Guglielmelli, E.; Stieglitz, T.; Rossini, P. M.; Micera, S. Restoring natural sensory feedback in real-time bidirectional hand prostheses. *Sci. Transl. Med.* **2014**, *6* (222), 222ra19.

(6) Tee, B. C. K.; Chortos, A.; Berndt, A.; Nguyen, A. K.; Tom, A.; McGuire, A.; Lin, Z. L. C.; Tien, K.; Bae, W. G.; Wang, H. L.; Mei, P.; Chou, H. H.; Cui, B. X.; Deisseroth, K.; Ng, T. N.; Bao, Z. N. A skin-inspired organic digital mechanoreceptor. *Science* **2015**, *350* (6258), 313.

(7) Hammock, M. L.; Chortos, A.; Tee, B. C. K.; Tok, J. B. H.; Bao, Z. 25th Anniversary Article: The Evolution of Electronic Skin (E-Skin): A Brief History, Design Considerations, and Recent Progress. *Adv. Mater.* **2013**, *25* (42), 5997−6038.

(8) Ma, R.; Lee, J.; Choi, D.; Moon, H.; Baik, S. Knitted fabrics made from highly conductive stretchable fibers. *Nano Lett.* **2014**, *14* (4), 1944−1951.

(9) Zang, Y. P.; Zhang, F. J.; Di, C. A.; Zhu, D. B. Advances of flexible pressure sensors toward artificial intelligence and health care applications. *Mater. Horiz.* **2015**, *2* (2), 140−156.

(10) Segev-Bar, M.; Haick, H. Flexible Sensors Based on Nanoparticles. *ACS Nano* **2013**, *7* (10), 8366−8378.

(11) Lee, J.; Kim, S.; Lee, J.; Yang, D.; Park, B. C.; Ryu, S.; Park, I. A stretchable strain sensor based on a metal nanoparticle thin film for human motion detection. *Nanoscale* **2014**, *6* (20), 11932−11939.

(12) Wang, X.; Dong, L.; Zhang, H.; Yu, R.; Pan, C.; Wang, Z. L. Recent Progress in Electronic Skin. *Advanced Science* **2015**, *2* (10), 1500169.

(13) Wang, X.; Gu, Y.; Xiong, Z.; Cui, Z.; Zhang, T. Silk-Molded Flexible, Ultrasensitive, and Highly Stable Electronic Skin for Monitoring Human Physiological Signals. *Adv. Mater.* **2014**, *26* (9), 1336−1342.

DOI: 10.1021/acsami.7b01979
ACS Appl. Mater. Interfaces 2017, 9, 14911−14919

(14) Tian, H.; Shu, Y.; Wang, X.-F.; Mohammad, M. A.; Bie, Z.; Xie, Q.-Y.; Li, C.; Mi, W.-T.; Yang, Y.; Ren, T.-L. A Graphene-Based Resistive Pressure Sensor with Record-High Sensitivity in a Wide Pressure Range. *Sci. Rep.* **2015**, *5*, 8603.
(15) Bae, G. Y.; Pak, S. W.; Kim, D.; Lee, G.; Kim, D. H.; Chung, Y.; Cho, K. Linearly and Highly Pressure-Sensitive Electronic Skin Based on a Bioinspired Hierarchical Structural Array. *Adv. Mater.* **2016**, *28* (26), 5300−5306.
(16) Su, B.; Gong, S.; Ma, Z.; Yap, L. W.; Cheng, W. L. Mimosa-Inspired Design of a Flexible Pressure Sensor with Touch Sensitivity. *Small* **2015**, *11* (16), 1886−1891.
(17) Yao, H.-B.; Ge, J.; Wang, C.-F.; Wang, X.; Hu, W.; Zheng, Z.-J.; Ni, Y.; Yu, S.-H. A Flexible and Highly Pressure-Sensitive Graphene-Polyurethane Sponge Based on Fractured Microstructure Design. *Adv. Mater.* **2013**, *25* (46), 6692−6698.
(18) Wang, J.; Jiu, J. T.; Nogi, M.; Sugahara, T.; Nagao, S.; Koga, H.; He, P.; Suganuma, K. A highly sensitive and flexible pressure sensor with electrodes and elastomeric interlayer containing silver nanowires. *Nanoscale* **2015**, *7* (7), 2926−2932.
(19) Mannsfeld, S. C. B.; Tee, B. C. K.; Stoltenberg, R. M.; Chen, C. V. H. H.; Barman, S.; Muir, B. V. O.; Sokolov, A. N.; Reese, C.; Bao, Z. Highly sensitive flexible pressure sensors with microstructured rubber dielectric layers. *Nat. Mater.* **2010**, *9* (10), 859−864.
(20) Yao, S.; Zhu, Y. Wearable multifunctional sensors using printed stretchable conductors made of silver nanowires. *Nanoscale* **2014**, *6* (4), 2345.
(21) Choi, W.; Lee, J.; Kyoung Yoo, Y.; Kang, S.; Kim, J.; Hoon Lee, J. Enhanced sensitivity of piezoelectric pressure sensor with micro-structured polydimethylsiloxane layer. *Appl. Phys. Lett.* **2014**, *104* (12), 123701.
(22) Dagdeviren, C.; Su, Y.; Joe, P.; Yona, R.; Liu, Y.; Kim, Y. S.; Huang, Y.; Damadoran, A. R.; Xia, J.; Martin, L. W.; Huang, Y.; Rogers, J. A. Conformable amplified lead zirconate titanate sensors with enhanced piezoelectric response for cutaneous pressure monitoring. *Nat. Commun.* **2014**, *5*, 4496.
(23) Pan, L.; Chortos, A.; Yu, G.; Wang, Y.; Isaacson, S.; Allen, R.; Shi, Y.; Dauskardt, R.; Bao, Z. An ultra-sensitive resistive pressure sensor based on hollow-sphere microstructure induced elasticity in conducting polymer film. *Nat. Commun.* **2014**, *5*, 3002.
(24) Jung, S.; Kim, J. H.; Kim, J.; Choi, S.; Lee, J.; Park, I.; Hyeon, T.; Kim, D. H. Reverse-micelle-induced porous pressure-sensitive rubber for wearable human-machine interfaces. *Adv. Mater.* **2014**, *26* (28), 4825−30.
(25) Mata, A.; Fleischman, A. J.; Roy, S. Characterization of polydimethylsiloxane (PDMS) properties for biomedical micro/nanosystems. *Biomed. Microdevices* **2005**, *7* (4), 281−293.
(26) McAlpine, M. C.; Ahmad, H.; Wang, D.; Heath, J. R. Highly ordered nanowire arrays on plastic substrates for ultrasensitive flexible chemical sensors. *Nat. Mater.* **2007**, *6* (5), 379−384.
(27) Wang, T.; Wang, R.; Cheng, Y.; Sun, J. Quasi In Situ Polymerization To Fabricate Copper Nanowire-Based Stretchable Conductor and Its Applications. *ACS Appl. Mater. Interfaces* **2016**, *8* (14), 9297−9304.
(28) Pang, C.; Lee, G. Y.; Kim, T. I.; Kim, S. M.; Kim, H. N.; Ahn, S. H.; Suh, K. Y. A flexible and highly sensitive strain-gauge sensor using reversible interlocking of nanofibres. *Nat. Mater.* **2012**, *11* (9), 795−801.
(29) Gong, S.; Schwalb, W.; Wang, Y.; Chen, Y.; Tang, Y.; Si, J.; Shirinzadeh, B.; Cheng, W. A wearable and highly sensitive pressure sensor with ultrathin gold nanowires. *Nat. Commun.* **2014**, *5*, 1 DOI: 10.1038/ncomms4132.
(30) Park, J.; Lee, Y.; Hong, J.; Ha, M.; Jung, Y. D.; Lim, H.; Kim, S. Y.; Ko, H. Giant Tunneling Piezoresistance of Composite Elastomers with Interlocked Microdome Arrays for Ultrasensitive and Multimodal Electronic Skins. *ACS Nano* **2014**, *8* (5), 4689−4697.
(31) Schwartz, G.; Tee, B. C. K.; Mei, J.; Appleton, A. L.; Kim, D. H.; Wang, H.; Bao, Z. Flexible polymer transistors with high pressure sensitivity for application in electronic skin and health monitoring. *Nat. Commun.* **2013**, *4*, 1859.
(32) Choong, C.-L.; Shim, M.-B.; Lee, B.-S.; Jeon, S.; Ko, D.-S.; Kang, T.-H.; Bae, J.; Lee, S. H.; Byun, K.-E.; Im, J.; Jeong, Y. J.; Park, C. E.; Park, J.-J.; Chung, U. I. Highly Stretchable Resistive Pressure Sensors Using a Conductive Elastomeric Composite on a Micro-pyramid Array. *Adv. Mater.* **2014**, *26* (21), 3451−3458.
(33) Tee, B. C. K.; Chortos, A.; Dunn, R. R.; Schwartz, G.; Eason, E.; Bao, Z. Tunable Flexible Pressure Sensors using Microstructured Elastomer Geometries for Intuitive Electronics. *Adv. Funct. Mater.* **2014**, *24* (34), 5427−5434.
(34) Fan, F.-R.; Lin, L.; Zhu, G.; Wu, W.; Zhang, R.; Wang, Z. L. Transparent Triboelectric Nanogenerators and Self-Powered Pressure Sensors Based on Micropatterned Plastic Films. *Nano Lett.* **2012**, *12* (6), 3109−3114.
(35) Wei, Y.; Chen, S.; Lin, Y.; Yang, Z. M.; Liu, L. Cu-Ag core-shell nanowires for electronic skin with a petal molded microstructure. *J. Mater. Chem. C* **2015**, *3* (37), 9594−9602.
(36) Chortos, A.; Bao, Z. Skin-inspired electronic devices. *Mater. Today* **2014**, *17* (7), 321−331.
(37) Niu, Z.; Gao, F.; Jia, X.; Zhang, W.; Chen, W.; Qian, K. Synthesis studies of sputtering TiO2 films on poly(dimethylsiloxane) for surface modification. *Colloids Surf., A* **2006**, *272* (3), 170−175.
(38) Couty, M.; Nazeer, S.; Jelita, C.; Martincic, E.; Woytasik, M.; Ginefri, J. C.; Darrasse, L.; Tatoulian, M.; Dufour-Gergam, E. Fabrication of metallic patterns on polydimethylsiloxane using transfer technology: application to MRI microcoils. *Micro Nano Lett.* **2012**, *7* (6), 519.
(39) Dinh, T. H. N.; Martincic, E.; Dufour-Gergam, E.; Joubert, P. Y. Capacitive flexible pressure sensor: microfabrication process and experimental characterization. *Microsyst. Technol.* **2016**, *22* (3), 465−471.
(40) Nichols, W. W. Clinical measurement of arterial stiffness obtained from noninvasive pressure waveforms. *Am. J. Hypertens.* **2005**, *18* (1 Pt 2), 3S−10S.
(41) Cai, F.; Yi, C.; Liu, S.; Wang, Y.; Liu, L.; Liu, X.; Xu, X.; Wang, L. Ultrasensitive, passive and wearable sensors for monitoring human muscle motion and physiological signals. *Biosens. Bioelectron.* **2016**, *77*, 907−913.
(42) Park, J.; Kim, M.; Lee, Y.; Lee, H. S.; Ko, H. Fingertip skin−inspired microstructured ferroelectric skins discriminate static/dynamic pressure and temperature stimuli. *Sci. Adv.* **2015**, *1*, e1500661.

DOI: 10.1021/acsami.7b01979
ACS Appl. Mater. Interfaces 2017, 9, 14911−14919